Applied Geochemistry 65 (2016) 14–21

Contents lists available at ScienceDirect

Applied Geochemistry

journal homepage: www.elsevier.com/locate/apgeochem

Iodine-129 chronological study of brines from an Ordovician paleokarst reservoir in the Lunnan oilfield, Tarim Basin

Jian Chen [a], Dayong Liu [a], Ping'an Peng [a, *], Chen Ning [b], Hou Xiaolin [b], Zhang Baoshou [c], Xiao Zhongyao [c]

[a] State Key Laboratory of Organic Geochemistry, Guangzhou Institute of Geochemistry, Chinese Academy of Sciences, 511 Kehua Street, Guangzhou, Guangdong 510640, China
[b] Xi'an AMS Center and State Key Laboratory of Loess and Quaternary Geology, Institute of Earth Environment, Chinese Academy of Sciences, Xi'an 710075, China
[c] Tarim Oilfield Company, PetroChina, Kuerle 841000, China

ARTICLE INFO

Article history:
Received 10 April 2015
Received in revised form
17 October 2015
Accepted 31 October 2015
Available online 4 November 2015

Keywords:
Iodine
Iodine 129
Oilfield water
Tarim basin

ABSTRACT

Previous studies have shown that brines in an Ordovician paleokarst reservoir of the Lunnan oilfield in the Tarim Basin, China, are the product of mixing of paleo-evaporated seawater in the east with paleometeoric waters in the west. In order to put time constraints on the brine and related hydrocarbons in this field, 10 brine samples were collected, for which the iodine concentrations and $^{129}I/I$ ratios were measured and discussed. The iodine concentration (3.70–31.2 mg/L) and the $^{129}I/I$ ratio (189 -897×10^{-15}) show that the iodine in the paleoseawater and meteoric water (MW) had different origins and ^{129}I characteristics. The paleoseawater has a high iodine content (~31 mg/L), indicating that iodine was introduced into the reservoir along with thermally generated hydrocarbons, possibly in the Cretaceous, from the Caohu Sag in the eastern area. Based on consideration of all possible origins of iodine and ^{129}I in the brines, it is suggested that the meteoric water maintained its initial iodine content (0.01 mg/L) and $^{129}I/I$ ratio (1500×10^{-15}), whereas the iodine-enriched paloseawater (IPSW) exhibited a secular ^{129}I equilibrium ($N_{sq} = 39$ atom/μL) as a result of fissiogenic ^{129}I input in the reservoir over a long period of time. The model of brine evolution developed on that basis confirmed that meteoric water entered the reservoir in the Miocene at about 10 Ma, and partially mixed with the iodine-enriched paleoseawater. The movement of meteoric water was facilitated by faults created during the Himalayan orogeny, then became more dense after dissolving Paleogene halite and infiltrated into the reservoir at high pressure. The iodine and ^{129}I concentration in the brine contains information about the path and history of the fluid in the reservoir. This may be useful in oil exploration, since the movement of water was, to some extent, related to hydrocarbon migration.

1. Introduction

Iodine is a liquid-dominated species since it is water soluble and its large ionic radius (133 pm) precludes it from being readily incorporated into minerals (Osborn et al., 2012). It is also strongly biophilic, and often accumulates in marine organic matter (10–490 ppm: Muramatsu and Wedepohl, 1998; 4.8–320 ppm: Muramatsu et al., 2004) by more than 100 times than that in sea water (0.05 ppm). As crude oils have a low iodine content (1 ppm: Fehn et al., 1987; 0–50 ppb: Moran et al., 1995b; 0.1–10 ppm: Worden, 1996), it is assumed that iodine is released into adjacent groundwater during maturation of organic matter in the source rock (Fehn, 2012); thus iodine enrichment in brines serves as a proxy for hydrocarbon migration.

Iodine-129 (^{129}I, $t_{1/2} = 15.7$ Myr) is the only long-lived radioisotope of iodine. Generally, there are three main sources of ^{129}I: (i) cosmogenic ^{129}I produced by the spallation of Xe isotopes into the atmosphere; (ii) fissiogenic ^{129}I produced by spontaneous fission of ^{238}U in the Earth's crust; and (iii) anthropogenic ^{129}I produced by nuclear weapons testing and fuel processing since the 1950s (Fehn,

* Corresponding author.
E-mail addresses: chenjian@gig.ac.cn (J. Chen), liudayong@gig.ac.cn (D. Liu), pinganp@gig.ac.cn (P. Peng), chenning@ieecas.cn (C. Ning), houxl@ieecas.cn (H. Xiaolin), zhangbaos-tlm@petrochina.com.cn (Z. Baoshou), xiaozhongy-tlm@petrochina.com.cn (X. Zhongyao).

http://dx.doi.org/10.1016/j.apgeochem.2015.10.012
0883-2927/

2012). In terms of these three sources, ^{129}I analysis has been successfully used for tracing and/or dating the fluids in a variety of geological settings, such as surface water and groundwater (Schwehr et al., 2005), hydrothermal fluids (Fehn et al., 1992), basinal brine (Osborn et al., 2012) and deep crustal fluids (Fehn and Snyder, 2005). Analysis of ^{129}I has also been used to trace waters associated with hydrocarbons in order to fix the age boundaries of organic accumulations (e.g., brines in oilfields: Birkle, 2006; gas hydrate: Fehn et al., 2000, 2003; forearc methane fields: Muramatsu et al., 2001; coalbed methane: Snyder and Fabryka-Martin, 2007; Snyder et al., 2003). While in these cases, the identification of the potential source formations was the main goal, iodine dating might help to determine mixing patterns and timing of brines in the Lunnan oilfield.

The target of the present study was the Ordovician paleokarst reservoir in the Lunnan oilfield located in the northern Tarim Basin. It is one of the major petroleum producers in that area (Fig. 1). The reservoir is deeper than 5000 m below sea level (mbsl) and is well known for its range of hydrocarbons, its weak intrareservoir connectivity and the tilted oil–water contact. These characteristics may be attributed to the multiple episodes of oil migration, evolution of the karst system, blending of different fluids and complex tectonic activity (Lu et al., 2004; Pang et al., 2007; Yang and Han, 2008; Zhang et al., 2011b).

Previous work on water chemistry and isotopes reached the following conclusions: (i) the brines in the reservoir are mixtures of infiltrated meteoric water at the top of the Lunnan Uplift with rising paleoseawater from the underlying marine strata in the Caohu Sag in the eastern area; (ii) the eastern fluid regimes are chemically separate from the western fluid regimes due to the larger contribution of the meteoric waters (Fig. 1); and (iii) two tentative hypothetical models of brine evolution were proposed (Chen et al., 2013).

Nevertheless, the geological periods in which these waters invaded remain unresolved. It is unclear whether the meteoric water is related to the period of karst development, or was intruded in a late basin uplift period. Furthermore, since the paleoseawater was derived from Cambrian and Lower Ordovician strata in the Caohu Sag, which itself is overlain by Middle–Upper Ordovician source rock, the important question remains as to whether paleoseawater migrated with the generated petroleum. The aims of our study are putting the time constraints on the brine and related hydrocarbons using ^{129}I isotopes as well as iodine concentrations.

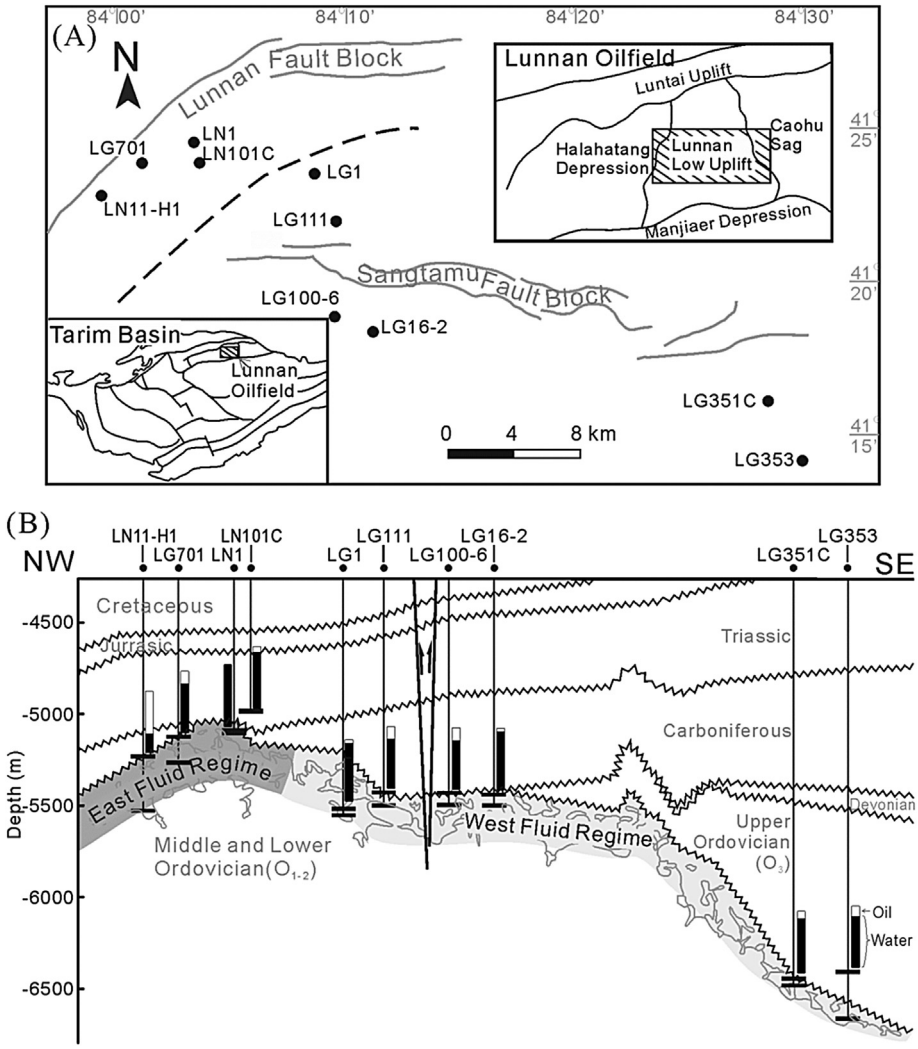

Fig. 1. (A) Study area and location of sampling wells in Lunnan oilfield, Tarim Basin, China. Insets in Fig. 1A are the structural maps of Tarim Basin and Lunnan oilfield. (B) Strata profile from Well LN11-H1 to Well LG353. Note: the oil/water volume ratios are shown in the short columns. Two fluid regimes are divided by dashed line in Fig. 1A and by different colors in Fig. 1B. Reprinted and modified from Chen et al. (2013) by permission from John Wiley and Sons.

2. Sampling and measurements

2.1. Geological background

The Lunnan oilfield, also known as the Lunnan Low Uplift, is located at the center of the Tabei Uplift in the northern part of Tarim Basin (Fig. 1A). It is surrounded by the Luntai Uplift, the Caohu Sag and the Manjiaer and Halahatang Depressions. Briefly, the local depositional environments may be divided into marine (Cambrian–Silurian), transitional (Carboniferous–Permian) and continental (Triassic–Quaternary) types, and the strata correspondingly evolved from limestone and dolomite to sandstone and mudstones. The tectonic evolution of the Lunnan oilfield can be divided into four periods (Zhao et al., 2007). Among them, two extensive tectonic movements—the Hercynian and Indo-Chinese orogenies (late Paleozoic–early Mesozoic)—exposed Middle–Lower Ordovician carbonate strata, which evolved into a karst systeme that significantly improved the physical properties of the present-day reservoir. Two sets of oil source rocks (Middle–Upper Ordovician and Lower Cambrian) are well reported in this region; oil source rocks younger than Ordovician do not occur. The detailed geological settings can be found in Chen et al. (2013), Wu et al. (2013) and Yang and Han (2008).

2.2. Sampling

In connection with previous water chemistry studies, between September 2009 and June 2010 the authors collected 37 brine samples in the target area (Chen et al., 2013). For the present study, 10 oilfield water samples of 1–2 L volume were selected for measurement of the iodine concentration and $^{129}I/I$ ratio. Nine of these were collected at depths between 5038 and 6667 mbsl in the paleokarst reservoir at the top of the Middle–Lower Ordovician carbonate strata (Fig. 1B). The other sample (LN101C) was taken from the Triassic reservoir at depths between 4984 and 4984.5 mbsl. The Ordovician samples lay within the typical karst interval (within 300 m: Gu, 1999; Pang and Shi, 2008), with the exception of one sample, LG1, which was deeper (within 320–360 m).

2.3. Measurements

The ionic, molecular and isotopic compositions of the 10 brines described in subsection 2.2 were reported by Chen et al. (2013). In the present work, only the iodine concentrations and $^{129}I/I$ ratios of these brines have been measured. The iodine concentrations were determined using a Thermal Electron Corporation X series II inductively coupled plasma mass spectrometer (ICP-MS). Replicate analyses yielded a precision better than 10%.

The samples for analyses by accelerator mass spectrometer (AMS) were prepared by the four-step procedure of $NaNO_2$ oxidation, CCl_4 extraction, $NaHSO_3$ back-extraction and $AgNO_3$ precipitation. The $^{129}I/I$ ratios in the recovered AgI were measured by AMS using a 3 MV tandem AMS system (HVEE), located in the Xi'an AMS Center. Details of the separation and measurement methods have been reported elsewhere (Chen et al., 2014; Zhou et al., 2013). Sample locations are shown in Fig. 1. The chemical and isotopic data are listed in Table 1.

3. Results and discussion

3.1. Iodine concentration and brine origin

Since chlorine and bromine are commonly considered to be conservative elements in fluids, the I–Cl and I–Br plots shown in Fig. 2 assist in investigating the source of the iodine. Unlike other ions, relatively few minerals in sedimentary basins have I and Br as major constituents (Hanor, 1994; Kharaka and Hanor, 2007; Worden, 1996). Chlorine is only affected by salt precipitation and dissolution; bromine may be slightly concentrated when the fluids are in contact with organic matter.

Iodine concentrations ranged between 3.70 and 31.2 mg/L, which is basically consistent with reports in the literature for formation waters (Worden, 1996) and oilfield waters (Fehn, 2012). Fig. 2(A and B) shows that all samples lay above the seawater evaporation trajectory (SET) with a 10- to 30-fold enrichment. Such a high level of enrichment cannot be the result of seawater evaporation, halite dissolution or any process of mineral transformation (e.g., albitization of plagioclase, or dolomitization), but rather it is attributed to the presence of organic matter associated with the biophilic character of iodine (Fehn, 2012). The highest iodine concentration was found in LG351C (31.2 mg/L) in the deep easternmost strata, and the lowest was in LN101C (3.70 mg/L) in the shallow western strata. Such high concentrations of iodine in the eastern samples imply that it came from one end member: paleoseawater sourced from rocks in the Caohu Sag located east of the Lunnan oilfield (Chen et al., 2013). This water assimilated iodine from maturing organic matter, and was then expelled with hydrocarbon migration. The lower concentration of iodine in the western samples was the result of substantial dilution of iodine-enriched paleoseawater (IPSW) by meteoric waters (MW) containing relatively little iodine.

It is not clear whether the meteoric waters have obtained additional iodine content by mixing with other fluids on the ground surface or from the leaching of sedimentary rocks as it infiltrated downward. Considering that there are no organic-rich sediments younger than the Ordovician in the history of hydrocarbon generation in this basin, the latter process might not have occurred. Likewise, meteoric waters containing high levels of dissolved chlorine from Carboniferous or Paleogene evaporites (Chen et al., 2013) have caused the plotted samples in the eastern fluid regimes to shift to the right somewhat in Fig. 2A. Nevertheless, no iodine could be released in the halite dissolution process.

3.2. $^{129}I/I$ ratio and age determination

Of the three sources of ^{129}I (see section 1), firstly anthropogenic sources may be disregarded since no artificial contamination took place during the sampling, and modern meteoric water cannot yet have infiltrated to the sampling depths. The other two sources should both be taken into account in geological age determination, however.

Cosmogenic ^{129}I is calculated using the decay formula:

$$R = R_i exp(-\lambda_{129} t), \quad (1)$$

where R is the $^{129}I/I$ ratio of the sample; R_i is the initial $^{129}I/I$ ratio of surface water ($=1500 \times 10^{-15}$, Fehn et al., 2007); λ_{129} is the decay constant of ^{129}I ($=4.41 \times 10^{-8}$ yr^{-1}); and t is the elapsed time.

When fluids are isolated from surface water (either meteoric water or sea water), ^{129}I is no longer replenished and diminishes following the decay formula, which allows the determination of the time t of separation. After about 90 Ma, the $^{129}I/I$ ratio from cosmogenic input will be below the detection limit of AMS. As the material is gradually buried, however, input from fissiogenic ^{129}I becomes significantly important.

Fissiogenic ^{129}I is calculated using the approach defined by Fabryka-Martin et al. (1989):

Table 1
Results of geochemical analyses of brines from the Ordovician paleokarst reservoir in Lunnan oilfield, Tarim Basin.

Sample	Age	Internal depth (m)	Cl[a] (mg/L)	Br[a] (mg/L)	I (mg/L)	^{129}I/I (10^{-15})	^{129}I (atom/μL)	X_{IPSW}[b] (%)
LN11-H1	O_{1+2}	5209.5–5530	151,200	235	7.98	588 ± 38	21.9	25.6
LG701	O_{1+2}	5121.2–5262.5	132,300	198	8.95	588 ± 53	24.6	28.7
LN1	O_{1+2}	5038–5052	133,900	171	11.0	448 ± 27	23.0	35.3
LN101C	T	4984–4984.5	134,500	117	3.70	897 ± 112	15.5	11.8
LG1	O_{1+2}	5520–5555	123,000	274	14.4	292 ± 21	19.6	46.0
LG111	O_{1+2}	5429.5–5500	120,800	273	21.6	359 ± 32	36.1	69.1
LG100-6	O_{1+2}	5433.5–5475	121,600	268	26.3	317 ± 21	38.9	84.3
LG16-2	O_{1+2}	5478–5505	12,6400	268	16.4	586 ± 65	45.0	52.7
LG351C	O_{1+2}	6448.5–6486.5	75,070	205	31.2	189 ± 13	27.5	100.0
LG353	O_{1+3}	6411.7–6667	74,350	222	29.4	270 ± 19	37.1	94.3
Reference								
Seawater (SW)			18,800[c]	67[c]	0.06[c]	1500[f]	0.43	
Pre-anthropogenic meteoric water (MW)			18.46[d]	0.02[d]	0.01[e]	1500[f]	0.07	

[a] Chen et al. (2013).
[b] X_{IPSW} is the proportion of iodine-enriched paleoseawater (assuming LG351C represents this endmember, see text for details).
[c] GERM (2004).
[d] Tomaru et al. (2009).
[e] Zhang et al. (2011a).
[f] Fehn et al. (2007).

$$N_{129} = N_{238}\lambda_{238}Y_{129}\rho\left(E/P\right)(1 - exp(-\lambda_{129}t))\Big/\lambda_{129}, \quad (2)$$

where N_{129} is the number of ^{129}I atoms; N_{238} is the number of ^{238}U atoms; λ_{238} is the decay constant for spontaneous fission of ^{238}U (=8.5 × 10^{-17} yr^{-1}); λ_{129} is the decay constant for spontaneous fission of ^{129}I (=4.41 × 10^{-8} yr^{-1}); Y_{129} is the production rate of mass 129 of that process (= 0.0003); ρ is the rock density; E is the proportion of fissiogenic ^{129}I released from the rock; P is the effective porosity of the rock; and t is the time that fluids are in contact with the rock. Generally, both cosmogenic and fissiogenic sources should be considered together when interpreting ^{129}I/I values in geological situations.

The ^{129}I/I ratios in the present study were between 1.89 × 10^{-13} and 8.97 × 10^{-13}. Obviously, 'old' cosmogenic ^{129}I from Ordovician and underlying marine strata (>443 Ma) can be neglected. Meteoric water with iodine concentration of 0.01 mg/L and ^{129}I/I ratio of 1500 × 10^{-15} alone cannot produce such high iodine concentrations and ionic concentrations (most samples > 140 mg/L: Chen et al., 2013), therefore, it is unreasonable that all the ^{129}I in the samples were cosmogenic and contained only in meteoric water. Nor can simple mixing of meteoric water and iodine-enriched paleoseawater (IPSW)—assuming sample LG351C was the endmember—yield such ^{129}I/I values as are shown in Fig. 3.

All the values falling above the mixture line in Fig. 3 imply that either (i) extraneous iodine was added to the meteoric water, forcing the data to shift to the right, and/or (ii) an excess amount of ^{129}I was added to the fluids, forcing the data to shift upward. In theory, the meteoric water may have acquired foreign iodine (including ^{129}I) when it mixed with other fluids on the surface, in a similar fashion to that reported for the Atacama Desert of northern Chile (Álvarez et al., 2015; Pérez-Fodich et al., 2014). In that example, the tectonic uplift of the Andes produced a sufficiently high hydraulic potential of iodine-rich fluids in Jurassic marine sediments (Álvarez et al., 2015) to cause large-scale movement (>20 km) of groundwater, which finally mixed with meteoric water in the Atacama Desert. However, in the present case, no studies have supported the historical occurrence of this kind of extensive surface fluid movement. Another possible source of excess iodine is the groundwater in overlying sediments, which could have mixed with the infiltrating meteoric water. Organic-rich marine sediments (Fehn, 2012; Fehn et al., 2007), which are regarded as source

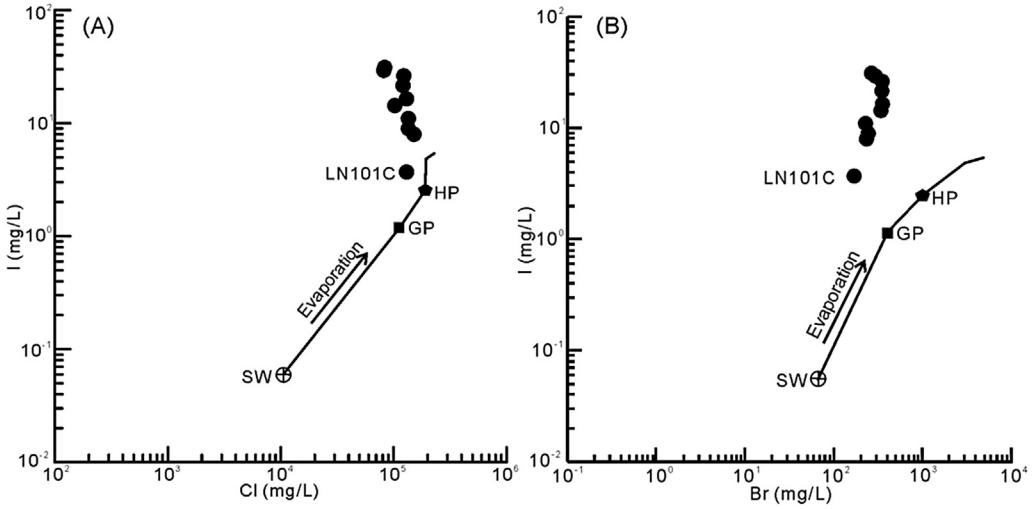

Fig. 2. (A) I vs. Cl relationship and (B) I vs. Br relationship of oilfield waters. The seawater evaporation trajectory (SET) was generated using data from GERM (2004) and Zherebtsova and Volkova (1966). GP = gypsum precipitaion; HP = halite precipitation.

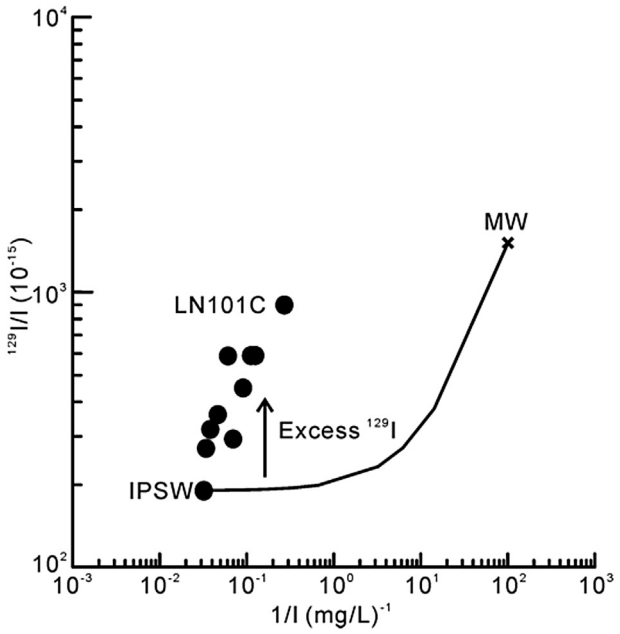

Fig. 3. Mixing diagram for 1/I vs. ^{129}I/I. Mixing is assumed to take place between iodine-enriched paleoseawater (IPSW, assuming LG351C represents this endmember) and meteoric water (MW). The data for the endmembers is listed in Table 1.

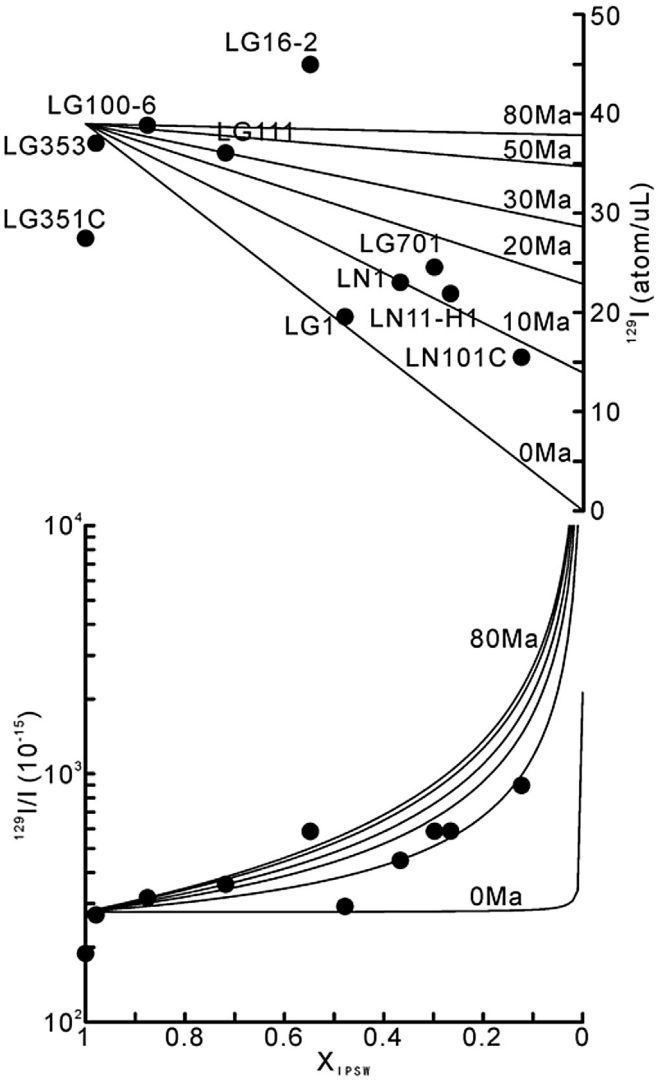

Fig. 4. Modeled effect of mixing different proportions of iodine-rich paleoseawater (IPSW) at secular equilibrium with meteoric water (MW) infiltrating downward at different times. The data for the endmembers is listed in Table 1.

rocks by petroleum geologists, are generally considered the source of iodine. In the Lunnan oilfield, the upper strata are transitional and terrestrial silicate rocks with a low total organic carbon (TOC) content, and certainly with a low iodine content. Also, it is expected that infiltrating meteoric waters would flow along narrow conduits such as faults; in which case, close contact between meteoric water and porewater in sedimentary strata is less likely, and therefore excess iodine take-up by meteoric water is unlikely to have occurred. Hence, excess ^{129}I may be the more likely reason for data shift from the mixing line in Fig. 3.

For the same reason, the presence of fissiogenic ^{129}I leached by meteoric water from overlying U-enriched mudstones and sandstones can be excluded indirectly. Only two potential fissiogenic ^{129}I sources might be responsible for the excess ^{129}I: (i) fissiogenic ^{129}I from underlying U-enriched source rocks; and (ii) in situ production of fissiogenic ^{129}I. Excess ^{129}I from paleoseawater expelled with hydrocarbon migration may also be excluded. Based on the reconstructed thermal maturation model, hydrocarbons were expelled from the Middle–Upper Ordovician source rocks in the Caohu Sag during the Cretaceous and early Tertiary (in fact > 100 Ma: Fig. 5 in Xiao et al., 2005). Even supposing that the paleoseawater obtained ^{129}I from the spontaneous fission of ^{238}U in the source rocks, most of it would have decayed in the subsequent 90 million years. Therefore, an in situ source seems to be the most probable.

To use Equation (2) to estimate the ^{129}I concentration in brine, values must be assigned to the parameters ρ, E and P. Carbonate density is 2.8 g/cm^3 (Fabryka-Martin et al., 1985) and U concentration is assumed to be 1–2 ppm or 2.5×10^{18}–5.0×10^{18} atom/kg, which is typical of carbonates (Becker et al., 1972; Fabryka-Martin et al., 1985). The E/P ratio is generally assumed to be between 1 and 3 (Fabryka-Martin et al., 1989; Liu et al., 1997; Moran et al., 1995a), but may be as high as 100 for granite (Fabryka-Martin et al., 1989) or volcanic rocks (Fehn et al., 1992) or metabasalt (Bottomley et al., 2002). Here, we have assumed $E/P = 10$, as the transport of ^{129}I into fluids may be quite efficient in carbonate rocks. The carbonate is readily dissolved and recrystallized in diagenesis. Visual and microscope observation indicated a considerable proportion of carved structures and cements (mainly calcite) in the samples, implying the occurrence of dissolution and recrystallization.

Similar mechanisms have been cited in the literature to explain the emanation of ^{129}I from rocks: Scholz et al. (2010) made reference to the mineral replacement and liquefaction process in explaining the origin of excess ^{129}I in brines in the Gulf of Cadiz, and Starinsky and Katz (2003) instanced the dissolution–precipitation model of granitic rocks to explain the formation of brines in Canadian Shield.

The value of N_{129} at secular equilibrium (>90 Ma) was calculated to be 39–78 atoms/μL.A true assessment of the ^{129}I source depends on the validity of the above values. To assign more precise values to the parameters, the U content in carbonate rocks needs to be investigated in the future, and the E/P ratio cannot be measured in the field. Nonetheless, the estimated value of 39–78 atoms/μL is higher than the values detected in this study, which suggests that in situ spontaneous fission of ^{238}U has the potential to produce and release enough ^{129}I into the brine, supporting our hypothesis regarding the source.

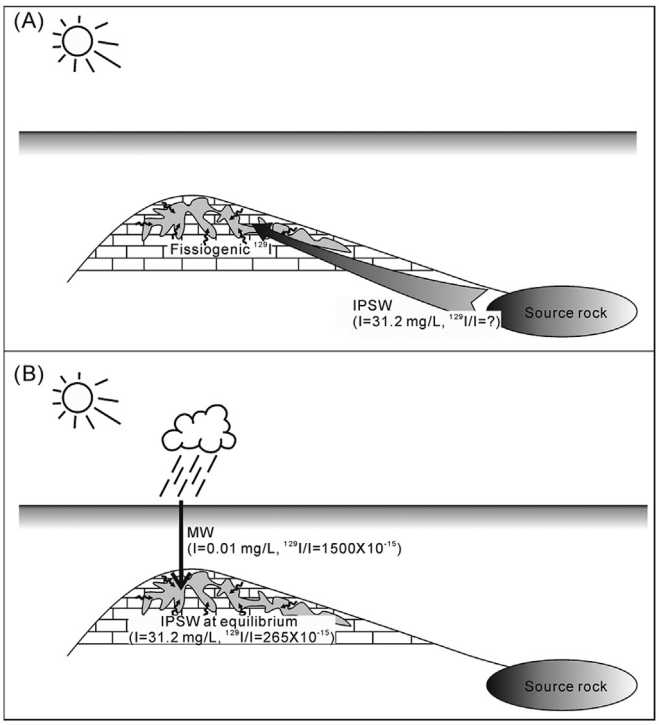

Fig. 5. Schematic diagram of brine evolution. (A) During the Cretaceous, iodine-enriched paleoseawater (IPSW) was expelled into the reservoir. (B) During the Miocene, meteoric water (MW) infiltrated downward to mix incompletely with paleoseawater at secular equilibrium.

With regard to paleoseawater which had entered the Ordovician reservoir before 100 Ma, it was found that three samples (LG353, LG100-6 and LG111) contained a high proportion of paleoseawater with similar ^{129}I values (37.1, 38.9 and 36.1 atom/μL, respectively). On that basis, the secular equilibrium value of ^{129}I in brine from in situ fissiogenic sources was assumed to be 39 atom/μL. Finally, the only remaining question is the time at which meteoric waters were introduced into the reservoir. Dilution of iodine-enriched paleoseawater by varying amounts of relatively iodine-depleted meteoric water in the past affect the current ^{129}I concentration as well as the ^{129}I/I ratio and the calculated ages, because meteoric water dilutes the original ^{127}I but has no effect on the in situ fissiogenic ^{129}I (Snyder and Fabryka-Martin, 2007). The implication is that the mixed N_{129} as a function of the proportion of paleoseawaters, X_{PSW}, and the time of the meteoric water entry, t, incorporates amounts from three separate contributors of ^{129}I to the meteoric water: (i) fissiogenic ^{129}I in paleoseawater at equilibrium, (ii) diminishing cosmogenic ^{129}I in meteoric water, and (iii) in-situ generated fissiogenic ^{129}I. The ^{129}I concentrations and ^{129}I/I ratios over time may be calculated from the following equations:

$$N_{129} = N_{sq}X_{PSW} + R_i exp(-\lambda_{129}t)N_{MW}(1-X_{PSW}) + N_{sq}(1-exp(-\lambda_{129}t))(1-X_{PSW}), \quad (3)$$

in which R is given by:

$$R = N_{129}/(N_{PSW}X_{PSW} + N_{MW}(1-X_{PSW})), \quad (4)$$

where N_{sq} is the secular equilibrium value (= 39 atom/μL); N_{MW} is the number of iodine atoms in meteoric water (= 0.01 mg/L = 4.74 × 10^{10} atom/μL, Table 1); N_{PSW} is the number of iodine atoms in paleoseawater, as represented by the brines in samples LG351C and LG353 (= 31 mg/L = 1.47 × 10^{14} atom/μL); and t is the time at which meteoric water entered the reservoir. The other parameters are as defined for Equations (1) and (2).

Most of the data falls along a line generated for 10 Ma (Fig. 4), suggesting that mixing occurred when meteoric waters intruded during the Miocene (~10 Ma). Some data (LG351C, LG16-2 and LG1) are off this line, perhaps related to the complicated fluid paths in the paleokarst. This reservoir is famous for its highly heterogeneous permeability (0.0001–748 × 10^3 μm^2) and porosity (0.15%–18.79%, Pang et al., 2007; Yang and Han, 2008). Carbonate rocks can eject more fissiogenic ^{129}I than other sedimentary rocks, but the heterogeneity of the karst reservoirs causes the ejection efficiency (E) to differ from well to well, and leads to the lesser accumulation of fissiogenic ^{129}I at some well locations (e.g., LG351C) but more enrichment elsewhere (e.g., LG16-2).

3.3. Infiltration of meteoric water into reservoir at 10 Ma

Meteoric water dating to 10 Ma is consistent with the existing tilted oil–water contact (Pang et al., 2007). Both facts indicate that the aquifer in this reservoir is still an active hydrodynamic environment, which may influence oil recovery. Although the occurrence of meteoric water in reservoirs up to 3000 mbsl is common (e.g., Birkle and Maruri, 2003; Grobe et al., 2000; Matray et al., 1994), in reservoirs as deep as the Lunnan oil field it has been observed only in one other case so far (Activo Luna oilfield, Gulf of Mexico, Birkle et al., 2002). Generally, the infiltration of meteoric water indicates that one or more of the following processes has occurred: high hydraulic pressure associated with a huge glacial sheet, or orogenic movement (Grasby and Betcher, 2000), or the development of fracture systems (Martini et al., 1998; Matray et al., 1994), or gravity-driven descent after waters suffered surficial evaporation (Birkle et al., 2002). Documented geological information indicates enhanced aridification, not glacial activity, in the Tarim Basin during the Cenozoic (Sun and Liu, 2006; Zheng et al., 2015), but the Himalayan Orogeny in this region was intense and peaked in the late Cenozoic along with the Tianshan Mountain uplift and Kuqa Depression in response to the collision of the Indian and Eurasian Plates (Zhang et al., 2011b, 2012; Zhu et al., 2013). The Himalayan Orogeny could have allowed the infiltration of meteoric water through faults, which then dissolved Paleogene lacustrine halite. Eventally, meteroic water arrived in the deep reservior and began to mix with palaeoseawater.

3.4. Improved brine evolution model

Based on the analyses of the iodine concentration and ^{129}I data in the brines, as well as earlier data (Chen et al., 2013), a more precise model of brine evolution is proposed as shown in Fig. 5:

(i) During the Cretaceous period, thermally generated hydrocarbons were expelled from marine Ordovician and Cambrian source rock in Caohu Sag. Iodine-enriched (~31 mg/L) paleoseawater (IPSW) entered the Ordovician paleokarst reservoir. The original concentration of ^{129}I in the paleoseawater subsequently diminished gradually over time, while fissiogenic ^{129}I was continuously injected as the product of radioactive decay of ^{238}U in the surrounding reservoir minerals and eventually the ^{129}I concentration in the brine reached secular equilibrium. For most samples, the equilibrium value was 39 atom/μL, although the value may differ in some wells.

(ii) At about 10 Ma (Miocene), meteoric water infiltrated downward into the structural high points of the reservoir through faults activated during the Himalayan orogeny. The present formation water in the Ordovician paleokarst

reservoir is the result of incomplete mixing of meteoric water having an initial iodine (0.01 mg/L) and $^{129}I/I$ ratio (1500×10^{-15}), and iodine-enriched paleoseawater (IPSW) at equilibrium ($N_{sq} = 39$ atom/μL).

4. Conclusion

As shown in above, the iodine-129 dating technique gives the opportunity to determine the mixing patterns and timing of paleoseawater and meteoric water in the Ordovician paleokarst reservoir of the Lunnan oilfield, Tarim Basin, China.

The east–west spatial trend of iodine and ^{129}I data has demonstrated the mixture of different fluids, which is consistent with previous research (Chen et al., 2013). The paleoseawater with high iodine content was derived from marine source rocks in the Caohu Sag and entered into the reservoir during the Cretaceous, when the source rocks reached their maximum oil generation. Subsequently, this formation water gained fissiogenic ^{129}I from the reservoir, eventually reaching secular ^{129}I equilibrium. The meteoric water with initial iodine and ^{129}I signatures invaded the high structural positions in the reservoir, and mixed incompletely with the iodine-enriched paleoseawater in the Miocene (about 10 Ma). Faults activated by intense tectonic movement during the Himalayan orogeny provided channels for the infiltrating meteoric water, and the dissolution of Paleogene evaporites produced an additional driving force.

We have shown here that ^{129}I contains information about fluid activities in complex reservoirs charged with waters from more than one source, which is useful knowledge for reducing costs and improving the efficiency of petroleum exploration.

Acknowledgments

This study was supported by the National Petroleum Project (Grant Number: 2011ZX05008-003) and the Natural Science Foundation of China (Grant Number: 41503051). We are very grateful to technicians in the Xi'an AMS Center and State Key Laboratory of Loess and Quaternary Geology, Institute of Earth Environment, Chinese Academy of Sciences, for the iodine-129 isotopic analyses. Thanks go to Prof. Michael Kersten, Dr. Peter Birkle and the anonymous reviewers for their critical comments, which greatly improved the quality of the manuscript.

References

Álvarez, F., Reich, M., Pérez-Fodich, A., Snyder, G., Muramatsu, Y., Vargas, G., Fehn, U., 2015. Sources, sinks and long-term cycling of iodine in the hyperarid Atacama continental margin. Geochim. Cosmochim. Acta. 161, 50–70.

Becker, V.J., Bennett, J.H., Manuel, O.K., 1972. Iodine and uranium in sedimentary rocks. Chem. Geol. 9, 133–136.

Birkle, P., 2006. Application of $^{129}I/^{127}I$ to define the source of hydrocarbons of the Pol-Chuc, Abkatún and Taratunich–Batab oil reservoirs, Bay of Campeche, southern Mexico. J. Geochem. Explor 89, 15–18.

Birkle, P., Maruri, R.A., 2003. Isotopic indications for the origin of formation water at the Activo Samaria–Sitio Grande oil field, Mexico. J. Geochem. Explor 78–79, 453–458.

Birkle, P., Aragon, J.J.R., Portugal, E., Aguilar, J.L.F., 2002. Evolution and origin of deep reservoir water at the Activo Luna oil field, Gulf of Mexico, Mexico. AAPG Bull. 86, 457–484.

Bottomley, D.J., Renaud, R., Kotzer, T., Clark, I.D., 2002. Iodine-129 constraints on residence times of deep marine brines in the Canadian Shield. Geology 30, 587–590.

Chen, N., Hou, X.L., Zhou, W.J., Fan, Y.K., Liu, Q., 2014. Analysis of low-level ^{129}I in brine using accelerator mass spectrometry. J. Radioanal. Nucl. Chem. 299, 1965–1971.

Chen, J., Liu, D.Y., Peng, P.A., Yu, C.L., Zhang, B.S., Xiao, Z.Y., 2013. The sources and formation processes of brines from the Lunnan Ordovician paleokarst reservoir, Tarim Basin, northwest China. Geofluids 13, 381–394.

Fabryka-Martin, J.T., Bentley, H., Elmore, D., Airey, P.L., 1985. Natural iodine-129 as an environmental tracer. Geochim. Cosmochim. Acta 49, 337–347.

Fabryka-Martin, J.T., Davis, S.N., Elmore, D., Kubik, P.W., 1989. In situ production and migration of ^{129}I in the Stripa granite, Sweden. Geochim. Cosmochim. Ac 53, 1817–1823.

Fehn, U., 2012. Tracing crustal fluids: applications of natural ^{129}I and ^{36}Cl. Ann. Rev. Earth Planet. Sci. 40, 45–67.

Fehn, U., Moran, J.E., Snyder, G.T., Muramatsu, Y., 2007. The initial $^{129}I/I$ ratio and the presence of 'old' iodine in continental margins. Nucl. Instrum. Methods B 259, 496–502.

Fehn, U., Peters, E.K., Tullai-Fitzpatrick, S., Kubik, P.W., Sharma, P., Teng, R.T.D., Gove, H.E., Elmore, D., 1992. ^{129}I and ^{36}Cl concentrations in waters of the eastern Clear Lake area, California: residence times and source ages of hydrothermal fluids. Geochim. Cosmochim. Ac 56, 2069–2079.

Fehn, U., Snyder, G.T., 2005. Residence times and source ages of deep crustal fluids: Interpretation of ^{129}I and ^{36}Cl results from the KTB-VB drill site, Germany. Geofluids 5, 42–51.

Fehn, U., Snyder, G., Egeberg, P.K., 2000. Dating of pore waters with ^{129}I: Relevance for the origin of marine gas hydrates. Science 289, 2332–2335.

Fehn, U., Snyder, G.T., Matsumoto, R., Muramatsu, Y., Tomaru, H., 2003. Iodine dating of pore waters associated with gas hydrates in the Nankai area, Japan. Geology 31, 521–524.

Fehn, U., Tullai, S., Teng, R.T.D., Elmore, D., Kubik, P.W., 1987. Determination of ^{129}I in heavy residues of two crude oils. Nucl. Instrum. Methods B 29, 380–382.

GERM, 2004. Geochemical Reference Model. http://earthref.Org/GERM/.

Grasby, S.E., Betcher, R., 2000. Pleistocene recharge and flow reversal in the Williston Basin, central North America. J. Geochem. Explor. 69–70, 403–407.

Grobe, M., Machel, H.G., Heuser, H., 2000. Origin and evolution of saline groundwater in the Münsterland Cretaceous Basin, Germany: Oxygen, hydrogen, and strontium isotope evidence. J. Geochem. Explor. 69–70, 5–9.

Gu, J.Y., 1999. Characteristics and evolutional model of karst reservoirs of Lower Ordovician carbonate rocks in Lunnan area of Tarim Basin (in Chinese). J. Palaeogeogr. 1, 54–60.

Hanor, J.S., 1994. Origin of saline fluids in sedimentary basins. In: Parnell, J. (Ed.), Geofluids: Origin, Migration and Evolution of Fluids in Sedimentary Basins. Geological Society of London Special Publication, pp. 151–174.

Kharaka, Y.K., Hanor, J.S., 2007. Deep fluids in the continents: I. Sedimentary basins. In: Drever, J.I. (Ed.), Treatise on Geochemistry: Surface and Ground Water, Weathering, and Soils. Elsevier-Pergamon, Oxford, pp. 1–48.

Liu, X., Fehn, U., Teng, R.T.D., 1997. Oil formation and fluid convection in Railroad Valley, NV: a study using cosmogenic isotopes to determine the onset of hydrocarbon migration. Nucl. Instrum. Methods B 123, 356–360.

Lu, H., Jia, W.L., Xiao, Z.Y., Sun, Y.G., Peng, P.A., 2004. Constraints on the diversity of crude oil types in the Lunnan Oilfield, Tarim Basin, NW China. Chin. Sci. Bull. 49, 19–26.

Martini, A.M., Walter, L.M., Budai, J.M., Ku, T.C.W., Kaiser, C.J., Schoell, M., 1998. Genetic and temporal relations between formation waters and biogenic methane: upper Devonian Antrim Shale, Michigan Basin, USA. Geochim. Cosmochim. Ac 62, 1699–1720.

Matray, J.M., Lambert, M., Fontes, J.C., 1994. Stable isotope conservation and origin of saline waters from the Middle Jurassic aquifer of the Paris Basin, France. Appl. Geochem. 9, 297–309.

Moran, J.E., Fehn, U., Hanor, J.S., 1995a. Determination of source ages and migration patterns of brines from the U.S. Gulf Coast basin using ^{129}I. Geochim. Cosmochim. Acta 59, 5055–5069.

Moran, J.E., Teng, R.T.D., Rao, U., Fehn, U., 1995b. Detection of iodide in geologic materials by high-performance liquid chromatography. J. Chromatogr. A 706, 215–220.

Muramatsu, Y., Fehn, U., Yoshida, S., 2001. Recycling of iodine in fore-arc areas: evidence from the iodine brines in Chiba, Japan. Earth Planet. Sci. Lett. 192, 583–593.

Muramatsu, Y., Wedepohl, K.H., 1998. The distribution of iodine in the earth's crust. Chem. Geol. 147, 201–216.

Muramatsu, Y., Yoshida, S., Fehn, U., Amachi, S., Ohmomo, Y., 2004. Studies with natural and anthropogenic iodine isotopes: Iodine distribution and cycling in the global environment. J. Environ. Radioact. 74, 221–232.

Osborn, S.G., McIntosh, J.C., Hanor, J.S., Biddulph, D., 2012. Iodine-129, $^{87}Sr/^{86}Sr$, and trace elemental geochemistry of northern Appalachian Basin brines: evidence for basinal-scale fluid migration and clay mineral diagenesis. Am. J. Sci. 312, 263–287.

Pang, W., Jiang, T.W., Zheng, J.M., Shi, H.X., 2007. Characteristics of the Ordovician buried hill reservoirs in Tahe-Lunnan oil area (in Chinese with English abstract). Oil Gas. Geol. 28, 762–767.

Pang, W., Shi, H.X., 2008. The paleo-karst feature of Ordovician carbonate rocks in Lunnan Area (in Chinese with English abstract). Xinj. Petrol. Geol. 29, 37–40.

Pérez-Fodich, A., Reich, M., Álvarez, F., Snyder, G.T., Schoenberg, R., Vargas, G., Muramatsu, Y., Fehn, U., 2014. Climate change and tectonic uplift triggered the formation of the Atacama Desert's giant nitrate deposits. Geology 42, 251–254.

Scholz, F., Hensen, C., Lu, Z., Fehn, U., 2010. Controls on the $^{129}I/I$ ratio of deep-seated marine interstitial fluids: 'Old' organic versus fissiogenic 129-iodine. EPSL 294, 27–36.

Schwehr, K.A., Santschi, P.H., Moran, J.E., Elmore, D., 2005. Near-conservative behavior of ^{129}I in the Orange County aquifer system, California. Appl. Geochem. 20, 1461–1472.

Snyder, G.T., Fabryka-Martin, J.T., 2007. ^{129}I and ^{36}Cl in dilute hydrocarbon waters: Marine-cosmogenic, in situ, and anthropogenic sources. Appl. Geochem. 22, 692–714.

Snyder, G.T., Riese, W.C.R., Franks, S., Fehn, U., Pelzmann, W.L., Gorody, A.W.,

Moran, J.E., 2003. Origin and history of waters associated with coalbed methane: ^{129}I, ^{36}Cl, and stable isotope results from the Fruitland Formation, CO and NM. Geochim. Cosmochim. Ac 67, 4529–4544.
Starinsky, A., Katz, A., 2003. The formation of natural cryogenic brines. Geochim. Cosmochim. Ac. 67, 1475–1484.
Sun, J.M., Liu, T.S., 2006. The age of the Taklimakan Desert. Science 312, 1621.
Tomaru, H., Lu, Z., Fehn, U., Muramatsu, Y., 2009. Origin of hydrocarbons in the Green Tuff region of Japan: ^{129}I results from oil field brines and hot springs in the Akita and Niigata Basins. Chem. Geol. 264, 221–231.
Worden, R.H., 1996. Controls on halogen concentrations in sedimentary formation waters. Mineral. Mag. 60, 259–274.
Wu, N., Cai, Z.X., Yang, H.J., Wang, Z.Q., Liu, X.F., Han, J.F., 2013. Hydrocarbon charging of the Ordovician reservoirs in Tahe-Lunnan area, China. Sci. China Ser. D. Earth Sci. 56, 763–772.
Xiao, X.M., Hu, Z.L., Jin, Y.B., Song, Z.G., 2005. Hydrocarbon source rocks and generation history in the Lunnan Oilfield area, Northern Tarim Basin (NW China). J. Pet. Geol. 28, 319–333.
Yang, H.J., Han, J.F., 2008. Accumulation characteristics and the main controlling factors of Lunnan multilayer oil province, Tarim Basin. Sci. China Ser. D. Earth Sci. 51, 65–76.
Zhang, L., Zhou, W., Hou, X., Chen, N., Liu, Q., He, C., Fan, Y., Luo, M., Wang, Z., Fu, Y., 2011a. Level and source of ^{129}I of environmental samples in Xi'an region, China. Sci. Total Environ. 409, 3780–3788.
Zhang, S.C., Zhang, B.M., Li, B.L., Zhu, G.Y., Su, J., Wang, X.M., 2011b. History of hydrocarbon accumulations spanning important tectonic phases in marine sedimentary basins of China: taking the Tarim Basin as an example. Pet. explor. Dev. 38, 1–15.
Zhang, S.C., Zhang, B., Yang, H.J., Zhu, G.Y., Su, J., Wang, X.M., 2012. Adjustment and alteration of hydrocarbon reservoirs during the Late Himalayan Period, Tarim Basin, NW China. Pet. explor. Dev. 39, 712–724.
Zhao, M.J., Pan, W.Q., Han, J.F., Liu, S.B., Qin, S.F., Zhang, B.M., 2007. Accumulation process and model for the Ordovician buried hill reservoir in the western Lunnan area, the Tarim Basin. Chin. Sci. Bull. 52, 224–235.
Zherebtsova, I.K., Volkova, N.N., 1966. Experimental study of behavior of trace elements in the process of natural solar evaporation of Black Sea water and Sasyk-Sivash brine. Geochem. Int. 3, 656–670.
Zheng, H.B., Wei, X.C., Tada, R., Clift, D.P., Wang, B., Jourdan, F., Wang, P., He, M.Y., 2015. Late Oligocene-early miocene birth of the Taklimakan desert. PNAS 112, 7662–7667.
Zhou, W.J., Chen, N., Hou, X.L., Zhang, L.Y., Liu, Q., He, C.H., Fan, Y.K., Luo, M.Y., Zhao, Y.L., Wang, Z.W., 2013. Analysis and environmental application of ^{129}I at the Xi'an Accelerator Mass Spectrometry Center. Nucl. Instrum. Methods B 294, 147–151.
Zhu, G.Y., Su, J., Yang, H.J., Wang, Y., Fei, A.G., Liu, K.Y., Zhu, Y.F., Hu, J.F., Zhang, B.S., 2013. Formation mechanisms of secondary hydrocarbon pools in the Triassic reservoirs in the northern Tarim Basin. Mar. Pet. Geol. 46, 51–66.